Stanford Exploration Project, Report 92, November 12, 1997, pages 121–136

Stanford Exploration Project, Report 92, November 12, 1997, pages 121–136

Validation and update of 3-D velocity models by inversion of seismic and well-log data

Arnaud Berlioux[1]

keywords: *velocity, modeling, three-dimensional, ray tracing*

ABSTRACT

In this paper, I propose a new procedure for estimating the validity of 3-D velocity models combining seismic data and well-log information. The method I describe gives the best least-square 3-D model for the velocity. It has even more potential for determining how accurate a velocity model is by estimating a range of possible models and giving a measure of local uncertainty about the velocity. I propose to use a 3-D prestack seismic survey as well as the well-log curves available on the site of the survey to evaluate and update a 3-D velocity model. Performing 3-D velocity analysis on the 3-D prestack seismic data, I will get an initial velocity model. From the well-log information, I plan to extract velocities at the well locations. I will then employ two different approaches to derive an accurate 3-D velocity model. The first is based on the least-square inversion of the well-log-derived velocities and uses the seismic velocities as a constraint, by applying for a conjugate gradient method. The second approach is a simulation of the velocity at each node of the 3-D model, using a sequential Gaussian simulation algorithm based on a generalized least-square inverse technique (kriging). I also intend to estimate local and global uncertainties about the velocity model I have derived.

INTRODUCTION

Nowadays, methods of three-dimensional seismic analysis are part of every oil company's activity. The depth migration of 3-D seismic data has become mandatory, and interpreters feel more comfortable working on depth-converted images because of the complex geological structure of the subsurface of the oil fields under investigation. Any 3-D depth migration algorithm requires a velocity model in order to yield a depth image of the geology. The risk of drilling dry holes increases and the decision to implant production wells becomes difficult when that decision is based on the interpretation of images that have been depth-converted with an inaccurate, or

[1]**email:** arnaud@sep.Stanford.EDU

imprecise, velocity model. An exact knowledge of the velocity is therefore required prior to any attempt to convert seismic data in depth.

Because the geologic structures of oil reservoirs are usually relatively local features, their mapping by seismic methods may become less reliable when rapid lateral velocity variations occur in the area. For this study, I make the hypothesis that the Dix assumption (1955) applies, but I know that this hypothesis is violated when I take into consideration the lateral variability on velocity.

Previous work

Accurate estimation of the interval velocity and its lateral variations is one of the most problematic steps in seismic data processing. In conventional seismic processing, the interval velocity model is derived from the stacking velocities, which are determined by measuring the coherency of the reflections along hyperbolic trajectories. Hubral et al. (1980) have shown that this method is an approximation which is only valid for horizontally stratified media and slight variations in lateral velocity.

A common approach to obtaining a velocity model varying horizontally and vertically, $V(x, z)$, is reflection tomography, based on traveltime inversion. Many variations on reflection tomography have been tested in recent years. They usually differ in the choice and parametrization of the data and the model space. Toldi (1985) presented a method for inverting stacking velocities. Landa et al. (1988) proposed to produce a velocity depth model that maximizes some measure of the coherency computed along traveltime curves. Harlan (1989) compared estimated traveltime with that of picked horizons but he does not allow for strong velocity gradients. Van Trier (1990) and Etgen (1990) used residual migration to determine interval velocities. Biondi (**?**) used beam stacking in conjunction with prestack migration in iterative inversion schemes to estimate the velocity model. Reflection tomography is an expensive process that is not currently used on 3-D data.

One of the most difficult problems facing the seismic processing industry is how to incorporate additional sources of information such as well logs and geologic models into seismic imaging (Versteeg and Symes, 1994; Toldi, 1995). Several studies have shown that a strict layering approach does not describe the velocity structure adequately, but does provide a starting point (Hanson and Whitney, 1995).

PROPOSED APPROACH

I propose to use 3-D inversion of the seismic data to estimate a 3-D velocity model that matches the given well-log information and follows the trend of the seismic data. To do so, I plan to integrate a set of irregularly-spaced 1-D well-log velocity curves and a 3-D seismic stacking velocity cube to produce a 3-D velocity model. This approach combines the processing and geostatistical analysis of seismic and well-log data.

First, I plan to analyze and preprocess the well-log data from a particular seismic survey. Ideally, this step would require the following well-log curves: sonic log, gamma ray log, and checkshot. The gamma ray curve is very useful for interpreting the geology and defining where the major boundaries separating the geological macro-layers are. If the sonic log is not available, it can be inferred from the gamma ray curve at the same well location. The sonic curve, along with a checkshot, will allow me to estimate the seismic (stacking) velocities at the well.

I will then process the 3-D seismic data in order to determine an initial 3-D velocity model. This processing comprises noise filtering, sorting of the traces from shot gathers into common depth-point gathers (CMP), and velocity analysis. I also plan to apply normal moveout to the CMP gathers before stacking them and to perform a depth migration in order to get an initial depth image of the geology. This stacked and/or depth-migrated image will help me visualize boundaries of the geological macro-layers and the presence of structural features such as faults, folds, and diapirs. The macro-layers observed in the section will help me make visual correlations with the processed well-log data.

Following this processing sequence for both data sets, I will define an inversion scheme based on the seismic and the well-log data (the data space) in order to derive a corresponding 3-D velocity model (the model space). The initial scheme I propose is a least-square inversion method that minimizes the function

$$\Phi(m) \;=\; E(m) \;+\; \epsilon^2\, L(m) \tag{1}$$

where $E(m)$ measures the prediction error between the estimated 3-D velocity model m and the well-log-derived velocity that is linearly interpolated on a regular grid. The presence of $L(m)$, which measures the length of the model, ensures that the trend of the estimated model does not move far away from the trend of the seismic velocity:

$$\begin{aligned} E(m) &= (d_w - Lm)^T\, C_w^{-1}\, (d_w - Lm) \\ L(m) &= [A\,(m - m_0)]^T\, [A\,(m - m_0)] \end{aligned} \tag{2}$$

where d_w is the velocity data derived from the well, L is the linear interpolation operator, and C_w^{-1} is the inverse covariance matrix of the well velocity. A is a roughening operator, and m_0 is the initial model, which is the seismic velocity data mapped onto the model space by linear interpolation ($m_0 = L^T d_s$).

The factor ϵ determines the relative importance given to the prediction error and the model length, which is also the relative importance given to the well data over the seismic data in this scheme. I will use a prediction error filter (PEF) determined from the seismic data for the roughening operator A. The role of this PEF is to ensure that the global trend of the estimated model follows roughly that of the initial seismic velocity.

Another approach to this problem is that provided by geostatistics. Ultimately, I want to derive a measure of the global and local uncertainties about the estimated 3-D velocity model using sequential Gaussian simulation algorithm. The same algorithm can be applied to obtain an estimated 3-D velocity model by means of the well-log-derived velocity and the initial seismic velocity model. First I will calculate the histogram of the cumulative distribution function (cdf) of the well velocity V_w and the initial seismic velocity V_s. I will apply a normal score transform φ to transform these velocity values V_w and V_s into Ω_w and Ω_s, following a standard normal distribution $\mathcal{N}(0,1)$ (Deutsch and Journel, 1992). Then I will perform a sequential Gaussian simulation on the Ω values, as follows:

1. I will define a random path that visits all the grid locations once. At each location i, I will define a neighborhood around the location $\vec{x_i}$ to retain only a portion of the data points.

2. At the location $\vec{x_i}$, I will infer a covariance model from the spatial variability of the data.

3. I will then estimate $\omega^*_K(\vec{x_i})$, the best least-square estimated value of Ω at the location $\vec{x_i}$, and $\sigma^2_K(\vec{x_i})$, the variance of the conditional cumulative distribution function (ccdf) of the random function Ω. This estimation is realized by a kriging with a trend (KT) algorithm, which requires the covariance model infered at step 2. I plan to perform KT on the well velocities using the trend of the seismic velocities to constrain the estimation.

4. I will go to the next location and repeat steps 1 to 3 until all the $\omega(\vec{x_i})$ are simulated.

Finally, I plan to back transform all the simulated normal values ω into simulated values for the velocity V.

Performing this conditional simulation will allow me to determine a measure of local and global uncertainties about the estimated velocity model. To obtain L equally probable simulated images of the velocity model, I will use the best least-square estimated value $\omega^*_K(\vec{x_i})$ in step 3 as the mean of the ccdf at location $\vec{x_i}$, draw L simulated values $\omega^{(l)}(\vec{x_i})\quad l = 1, L$ based on the ccdf $\mathcal{N}(\omega^*_K(\vec{x_i}), \sigma^2_K(\vec{x_i}))$, and back transform them into the velocity space. At each location $\vec{x_i}$, the L simulated values provide a histogram of possible outcomes for that particular location, which is a model of local uncertainty about the velocity. In addition, for each of the L simulated images, I can average the simulated velocities over the entire space and organize the result in a histogram that provides a measure of global uncertainty about the average estimated velocity.

WORK COMPLETED

This section presents two data sets I worked on. I investigated the inversion technique using the conjuguate gradient method on a data set provided by Chevron Research Laboratory. The second data set, given by Pathfinder Oil and Gas, contained several well-log curves on which I did some preliminary preprocessing.

Chevron dataset

At the beginning of 1995, John Toldi from Chevron Research Laboratory in La Habra provided SEP with a sample of data extracted from a data set. The sample data comprise a series of isovelocity (average velocity) surfaces and a set of well data points. The surfaces are isovelocity maps extracted from a 3-D root mean-squared (RMS) velocity cube and converted into average velocity maps. These maps give the depth to a particular velocity (e.g., 2000 m/s) at different locations. The well data points give the depth at the well location where the same isovelocity surface has been observed. These well velocity values were calculated from checkshots. Both kinds of data were available as GOCAD surfaces. GOCAD (Mallet, 1994) is a software package that offers numerous tools for building, viewing, and manipulating geologic models described as surfaces. Figure 1 represents a plane view of the 2000 m/s seismic isovelocity map. The black squares correspond to the location of the well data values for the same isovelocity surfaces.

The ultimate goal of this study is the depth conversion of the original seismic data. The well-derived velocities represent an accurate, but poorly sampled, data set. The seismic velocity is much denser, but less accurate. The velocity at the well is a measurement (high resolution, one sample per foot) while the seismic velocity is derived by calculations relying on the seismic two-way traveltime. Also, the conventional processing of the seismic data does not account for anisotropy. The stacking slowness (inverse of the velocity) depends on the traveltime, which depends on the physical interval slowness. Therefore, any uncertainty regarding the interval slowness or traveltime will have an effect on the stacking slowness estimation. The seismic stacking velocity also has a bias as a depth predicter; that is, there is a systematic mistie between the seismic and the well data sets. My goal is to cancel or at least significantly reduce this mistie.

Prior to receiving this data set, I studied an identical problem with a synthetic data example (Berlioux, 1995). The approach I took was to address this problem with a least-squares inversion scheme defined with the following set of equations:

$$\begin{cases} 0 \approx L\,m - d_w \\ 0 \approx \epsilon\,A\,(m - m_0) \end{cases} \tag{3}$$

The first equation of (3) performs a mapping of the well data d_w by linear interpolation, L being the linear interpolation operator, onto the model space m. The second

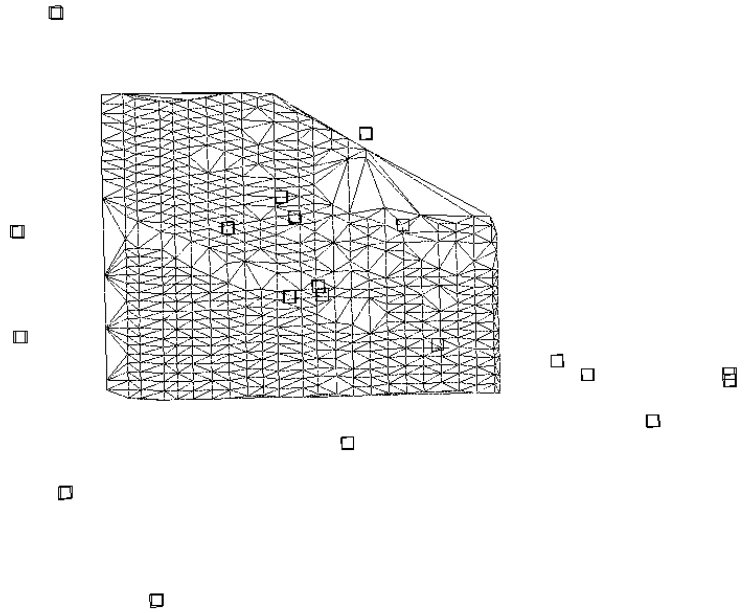

Figure 1: GOCAD model for the Chevron data set. The triangulated surface represents the seismic-derived 2000 m/s isovelocity surface. The black small cubes show the location of the well data values. arnaud-chevron-gocad [NR]

equation of (3) describes the minimization of the error between the model and the linearly interpolated seismic data as an initial version of the model. The scaling factor ϵ sets the relative importance of the well data over the seismic data. I use a PEF determined from the seismic data for the roughening operator A.

I solved the system of equations (3) by a conjugate gradient (CG) method. The CG approach produced good results for a synthetic example made of one isovelocity surface and four well data values. However, the same set of equations and the CG method did not produce conclusive results when applied to the Chevron data set. Figure 2 shows the 2000 m/s isovelocity surface after 1000 iterations of CG with a 5x5 PEF. High spikes are clearly visible around the well locations, and the depth to the surface is modified at the edge of the top right and lower left corner zones where no seismic data is available. I reduced the data set by extracting a portion of the same isovelocity map. These new data do not have the same disadvantages of the previews map, i.e., there is no jump at the edges to a zero value. Figure 3 shows the result of 1000 iterations of CG with a 5x5 PEF using the reduced data set. The resulting map is very smooth and follows the trend of the original seismic data. The misties at the well have been significantly reduced in general and cancelled for more than half the wells.

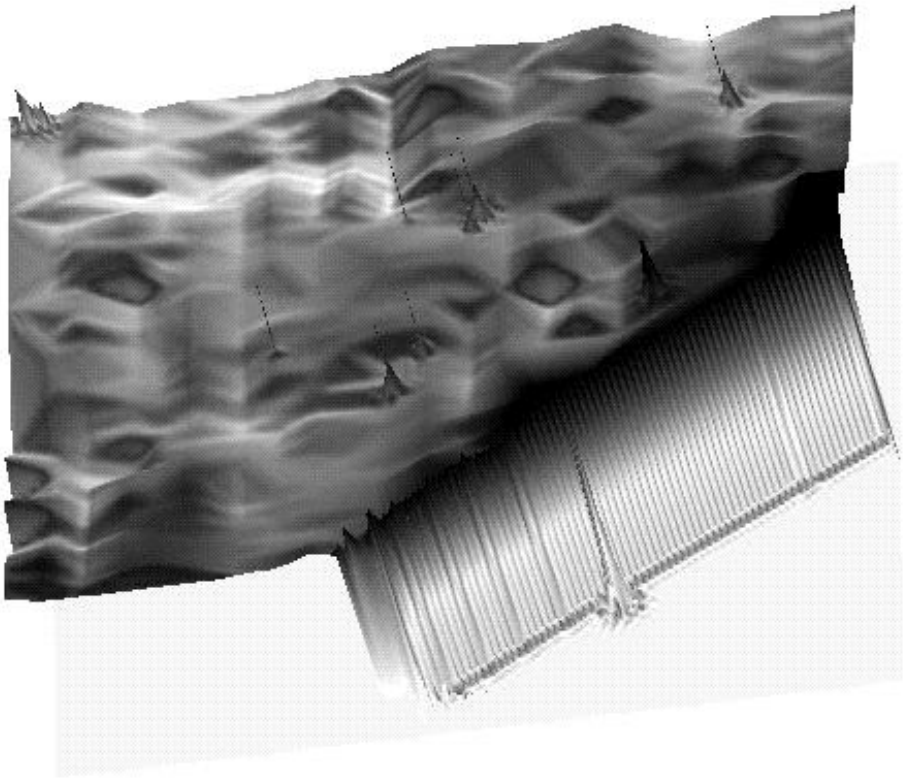

Figure 2: 2000 m/s isovelocity surface modeled by 1000 iterations of conjugate gradient with a 5x5 prediction error filter. The surface is viewed upside-down within AVS showing high spikes at the well locations (vertical exaggeration 100:1). arnaud-chevron-pef [NR]

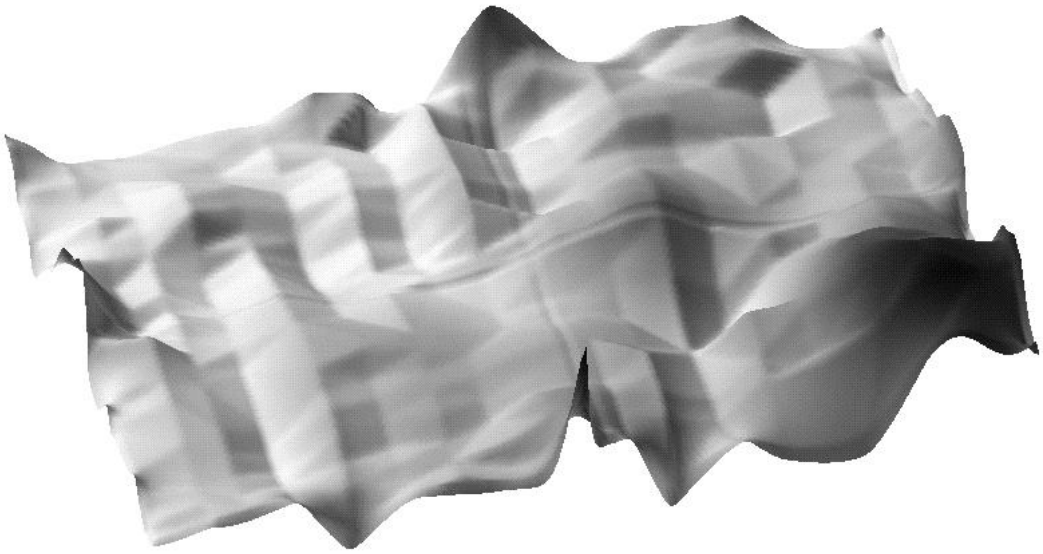

Figure 3: Portion of the 2000 m/s isovelocity surface modeled by 1000 iterations of conjugate gradient with a 5x5 prediction error filter. The misties at the well have been dramatically reduced, and the surface follows the trend of the original seismic data. arnaud-crop-pef [NR]

Pathfinder dataset

In October 1995, Pathfinder Oil and Gas, Inc., made available to me a portion of a 3-D land data set. The original prestack data set was recorded on an irregular, 17.5 square-mile grid. The sampling rate in time is 2 milliseconds over a 3 second total time recorded. There are 65 wells drilled on the site of the survey. The available data set comprises a poststack time-migrated 3-D seismic cube (3.6 squared miles) and six sets of well-log curves recorded at six different locations on the survey site. Figure 4 shows the interval velocity map for a particular horizon of the survey and the six well locations. The two southern wells (E and F) are dry holes.

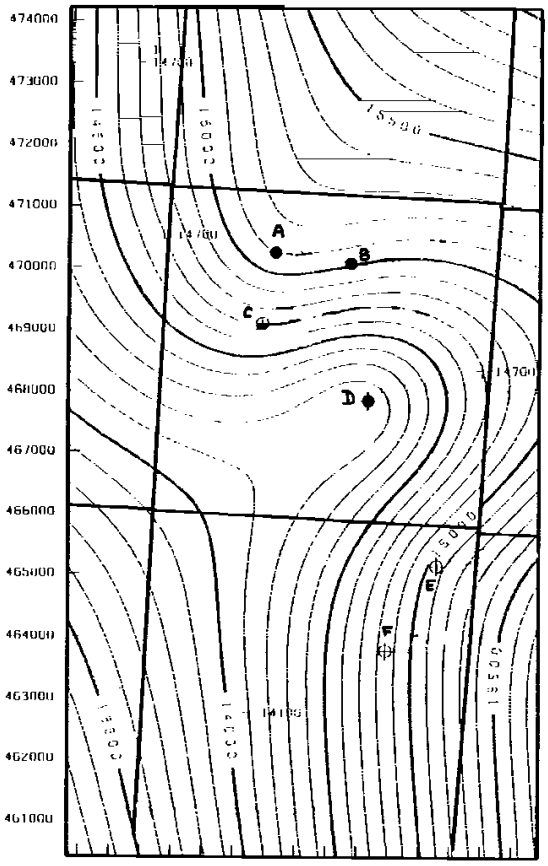

Figure 4: Interval velocity map for one of the main reflectors on the site of the survey. In the four wells at the center of the figure, oil has been observed, and two of them are producing oil. The wells E and F at the bottom of the figure are dry holes. arnaud-horizon [NR]

As of the date of this article, I have not received the corresponding 3-D prestack shot gathers and the stacking velocity model used to migrate the seismic data. I will also obtain four more well logs. The well-log curves available are two sonic logs, six gamma ray logs, as well as other curves (induction, self-potential, porosity, and density). No checkshots have been recorded in any of these wells.

The geology for the area is not structurally complex: at the depth of the target zone, the geology shows prograding carbonates and clastic sediments embedded in thin sand layers in a shaly environment. The prograding of the carbonated series makes it difficult to predict the extent of the oil reservoir reached by the four northern wells. Several dry holes have been drilled already in this area because of the inaccuracy of the velocity model used for the time-to-depth conversion.

For this data set I worked with the six well-log curves available. I blocked by hand all the gamma ray curves in order to do visual correlations between the various wells. I defined nine major interfaces on one curve and retrieved them on the five other curves. These interfaces bound regions of the curve where the gamma ray values are roughly constant (high-frequency oscillations around a mean value). I also blocked by hand the two sonic curves and retrieved the same nine interfaces as determined on the gamma ray. Figure 5 shows a portion of the sonic and gamma ray curves around the target zone. The high-frequency component of the original logs has been removed by median filtering on a running window. The four curves present strong similarities exploitable for interpretation and visual correlations. I then plotted several scattergrams showing the existence of a correlation between the sonic and the gamma ray curves at the two wells where both pieces of information were available. I also observed a strong correlation ($\rho_{linear} \geq 0.94$) between the blocked sonic and the gamma ray logs. Figure 6 shows this correlation on two scattergrams of sonic median filtered values plotted against gamma ray median filtered values for the nine layers defined around the target zone.

WORK TO BE DONE

In this section I describe in greater detail what still remains to be done in each step of the processing sequence.

Seismic data processing

One must carefully process seismic data in order to extract the stacking velocity information. Typically, the processing involves

- noise filtering, including static removal (land data), multiple suppression (marine data), and muting
- sorting of the shot gathers into CMP gathers, which can be tedious in the case of irregular 3-D geometry of acquisition
- velocity analysis, which yields a stacking velocity model
- NMO, stacking, time migration, and/or depth migration

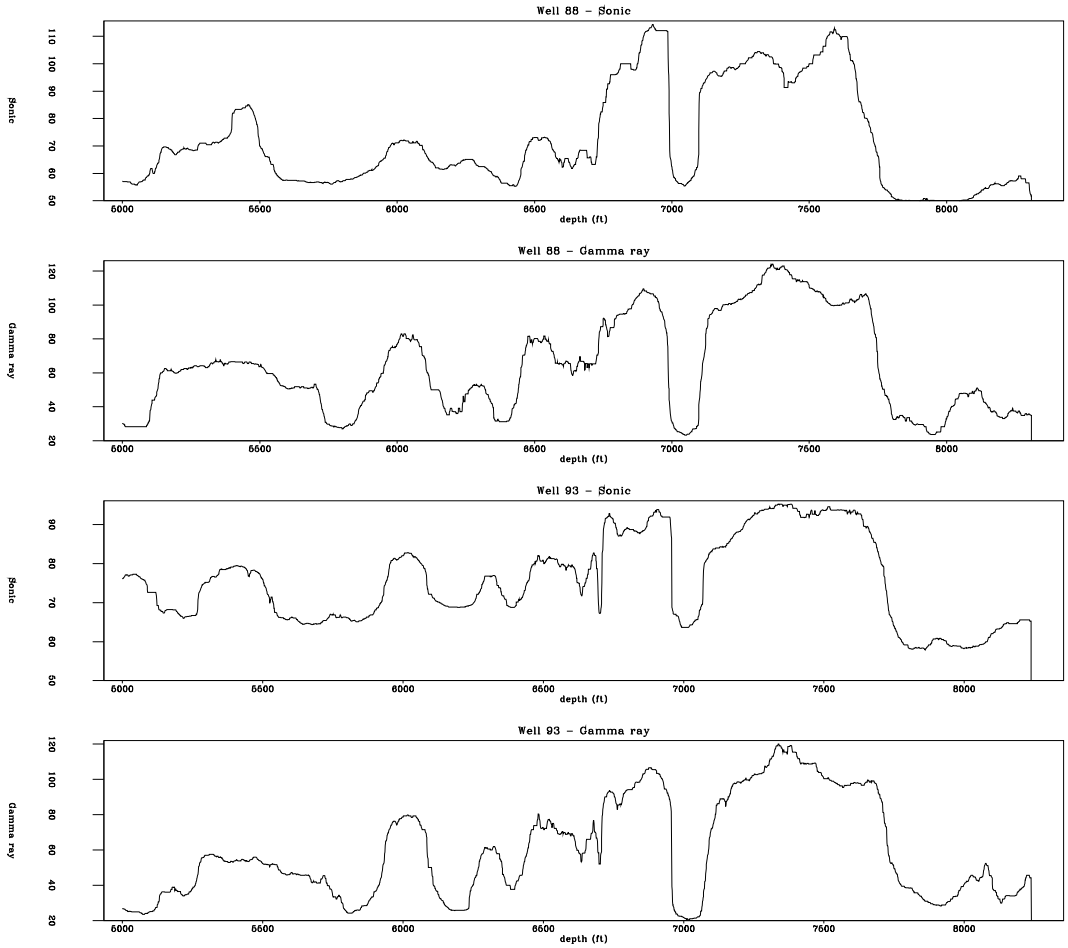

Figure 5: Sonic and gamma ray curves for wells E and F. The high-frequency component has been filtered out by median filtering on a running window. arnaud-dt-gr.88-93 [NR]

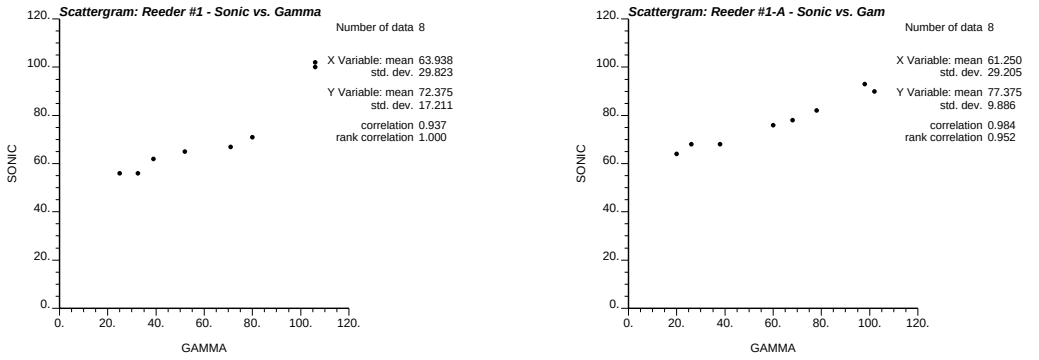

Figure 6: Scattergrams of sonic versus gamma ray values for nine layers around the target zone. arnaud-sub-dt-gr [NR]

I plan to perform the processing of the seismic data with PROMAX, as well as with SEP in-house programs.

Well-log data processing

The processing of the well-log data requires several steps that need to be automated. First, I will block the well-log curves to keep the low-frequency variations, thereby allowing definition of interfaces between the different facies. This step is the most important for this data type since it conditions the results obtained after further processing of the logs. The sonic logs and the gamma ray logs will be blocked as well. Other curves, such as the density log, may also require blocking.

Once the blocking has been performed, I will derive an interval velocity $V_{int}(i)$ within each block using either

- the direct summation from ray theory, as follows:

$$V_{int}(i) \;=\; \frac{\Delta Z_i}{\Delta T_i} \qquad \Delta T_i \;=\; \sum_j \delta t_j \tag{4}$$

  where ΔZ_i is the thickness of the block i and ΔT_i is the sum of all the sonic values δ_j within the block i, or

- the Backus average from effective medium theory:

$$\frac{1}{M_i} \;=\; \frac{1}{\Delta Z_i}\int \frac{dZ}{\rho v^2} \qquad V_{int}(i) \;=\; \sqrt{\frac{M_i}{\rho_i}} \tag{5}$$

  where ρ is given by the density log, v is given by the sonic log ($v = 1/\delta t$), and ρ_i is the average density, indicated by the blocked density log.

The choice of method depends on the ratio of the seismic data wavelength to the thickness of the block. Ray theory is used when this ratio is less than 10. When it is greater than 10, effective medium theory applies.

Using the Dix equation (1955) I can convert the interval velocity into RMS velocity, which is assumed to be the same as the stacking velocity.

Least-squares inversion

Although I have already written a Fortran77 program to solve a system of equations similar to (3) by the conjugate gradient method, Figure 2 shows that this program needs improvement in order to perform the inversion automatically without running into problems of edge effects.

The general procedure for estimating the velocity model will be to iterate until an acceptable velocity model is calculated, as follows:

- The mapping of the seismic velocity data onto the model space gives an initial guess of the model.
- The standard damped least-squares inversion is applied. At iteration k, I
  - first invert for the model perturbation

$$\delta m_k \;=\; \left[\epsilon^2 A^T A\right]^{-1} L^T C_w^{-1}(d_w \;-\; L m_k) \tag{6}$$

  - then update the velocity model

$$m_{k+1} \;=\; m_k \;+\; \delta m_k \tag{7}$$

The convergence is achieved when the mistie between the well velocity and the calculated velocities has been eliminated.

Sequential Gaussian simulation

I plan to use GSLIB (Deutsch and Journel, 1992) to perform both the kriging of the well velocity with the seismic velocity as a trend and the sequential Gaussian simulation (sGs) to calculate a measure of the local and global uncertainties about the estimated model.

The kriging estimated value of the velocity based on the well data and using the seismic velocity model as a linear trend is

$$V^*(\vec{x}) \;=\; \sum_{\alpha=1}^{N} \lambda_\alpha V(\vec{x}_\alpha) \tag{8}$$

where coefficients λ_α are estimated by solving the kriging with a trend (KT) system (9), and $V(\vec{x}_\alpha)$ are the velocities of the N neighboring points located at position $\vec{x}_\alpha$ used to determine $V^*(x)$. The KT system is made of $(N+3)$ equations:

$$\left\{ \begin{array}{lllllll} \sum_{\beta=1}^{N} \lambda_\beta C(\vec{x}_\alpha - \vec{x}_\beta) & + & a_0 & + & a_1 x_\alpha & + & a_2 y_\alpha \;=\; C(\vec{x}_\alpha - \vec{x}) \quad \alpha = 1, N \\ \sum_{\beta=1}^{N} \lambda_\beta & & & & & & \;=\; 1 \\ \sum_{\beta=1}^{N} \lambda_\beta x_\beta & & & & & & \;=\; x \\ \sum_{\beta=1}^{N} \lambda_\beta y_\beta & & & & & & \;=\; y \end{array} \right. \tag{9}$$

where $C(\vec{x}_\alpha - \vec{x}_\beta)$ is the covariance of the velocity at location $\vec{x}_\alpha$ and location $\vec{x}_\beta$, and a_i are the coefficients of the linear trend:

$$m(\vec{x_\alpha}) \;=\; a_0 \;+\; a_1 x_\alpha \;+\; a_2 y_\alpha \tag{10}$$

A covariance model is therefore needed and will be inferred from the semi-variogram $\gamma(h)$ model of the well velocity. By definition, $\gamma(h)$ is equal to $C(0) - C(h)$. The sGs will also allow me to estimate a range of equiprobable velocity models that will require some interpretation in order to produce a measure of the uncertainty about the estimated velocity model.

The sGs procedure is based on the normal score transform of the velocity random variable $V(\vec{x})$, assuming that the transformed variable is multi-normal. When the multi-normality hypothesis cannot be retained, I will use an indicator simulation instead of the Gaussian approach.

Visualization of the 3-D velocity model

I will use the GOCAD and AVS (Advanced Visual System) software packages to visualize the 3-D velocity models at each stage of this project. The combination of both software packages has proven particularly efficient in rendering 3-D models easily and accurately, which is essential to understanding 3-D velocity structures (Biondi and van Trier, 1993; Clapp et al., 1994).

REFERENCES

Berlioux, A., 1995, Tying well information and seismic data: SEP–**84**, 319–324.

Biondi, B., and van Trier, J., 1993, Visualization of multi-dimensional seismic dataset with cm-avs: SEP–**79**, 1–12.

Clapp, R. G., Biondi, B., and Karrenbach, M., 1994, AVS as a 3-D seismic data visualizing platform: SEP–**82**, 97–106.

Deutsch, C. V., and Journel, A. G., 1992, GSLIB Geolstatistical Software Library and User's Guide: Oxford University Press.

Dix, C. H., 1955, Seismic velocities from surface measurements: Geophysics, **20**, no. 1, 68–86.

Etgen, J., 1990, Interval velocity estimation for two-dimensional prestack depth migration: SEP–**68**, 83–100.

Hanson, D. W., and Whitney, S. A., 1995, 3D prestack depth migration - velocity model building and case history *in* Harlan, W. S., Ed., Seismic Depth Estimation:: Geophysical Society of Tulsa, 27–52.

Harlan, W. S., 1989, Tomographic estimation of seismic velocities from reflected raypaths: 59th Annual Internat. Mtg., Soc. Expl. Geophys., Expanded Abstracts, 922.

Hubral, P., and Krey, T., 1980, Interval velocities from seismic reflection traveltime measurements: Soc. Expl. Geophys., Tulsa.

Landa, E., Kosloff, D., Keydar, S., Koren, Z., and Reshef, M., 1988, A method for determination of velocity and depth from seismic reflection data: Geophys. Prosp., **36**, no. 3, 223–243.

Mallet, J. L., 1994, GOCAD Report, version 9.1, Confidential: Association Scientifique pour la Géologie et ses Applications.

Toldi, J., 1985, Velocity analysis without picking: SEP–**43**, 0–8.

Toldi, J. L., 1995, Combining velocity information from a variety of sources *in* Harlan, W. S., Ed., Seismic Depth Estimation:: Geophysical Society of Tulsa, 97–99.

van Trier, J., 1990, Tomographic determination of structural velocities from depth migrated seismic data: Ph.D. thesis, Stanford University.

Versteeg, R. J., and Symes, W. W., 1994, Geologic constraints on seismic inversion: 64th Annual Internat. Mtg., Soc. Expl. Geophys., Expanded Abstracts, 1020–1023.